ac conductivity and ac photoconductivity in amorphous and crystalline insulators

M. Abkowitz, A. Lakatos, and H. Scher
Xerox Rochester Research Center, Rochester, New York 14644
(Received 11 October 1973)

Measurements of ac conductivity and ac photoconductivity are reported on representative amorphous and crystalline insulators. Low-frequency measurements have been argmented by photomicrowave experiments. In the dark some of these materials exhibit the familiar ω^s frequency dependence but under illumination all materials studied exhibit frequency-independent ac conductivity in the range 20 Hz–100 kHz. The amorphous chalcogenides studied do not exhibit photomicrowave response; however, strong response is observed in these films following crystallization *in situ*. Frequency-independent ac conductivity is usually associated with transport in extended states. In As_2Se_3, however, transient measurements are interpreted most easily in terms of hopping transport. A phenomenological model which reconciles these observations is presented. Aspects of the relationship of steady-state ac to dc electrical measurements and the relationship of ac measurements to the time-of-flight technique are analyzed.

I. INTRODUCTION

Present interest in ac conductivity stems from the possibility that the phonon-assisted hopping of charge carriers among the localized states may be an important transport mechanism in amorphous and molecular solids. Characteristic frequency and temperature dependences of ac conductivity are predicted by the various hopping-transport models published to date.[1,2] Quite apart from this there has been increasing interest in developing techniques to measure the electrical properties of composite, polycrystalline, polymeric, and biological materials in a "contactless" configuration, for example, by microwave-perturbation techniques.[3]

We present here a study of dark and ac photoconductivity in some representative amorphous and crystalline solids. At low frequencies, ac conductivity is viewed largely as an extension of traditional dc electrical measurements, which now adds frequency to the more familiar parameters of such measurements. As the excitation frequency increases, contact effects and internal barriers become capacitatively short circuited and losses are expected to directly reflect bulk dissipative mechanisms. At a given frequency, however, the steady-state ac conductivity may represent the combined effect of several processes having distinctive frequency dependences. In amorphous chalcogenides the interplay of such processes is found to dominate the behavior of the ac photoconductivity and is shown to be responsible for our inability to observe microwave photoconductivity in this class of materials whereas it is readily observed in polycrystalline trigonal selenium.

A frequency-independent ac photoconductivity is characteristic of all solids investigated in the present study. While this is not a surprising feature of solids exhibiting well-defined band structure, transport in several of these materials is believed, on the basis of time-of-flight measurements, to be dominated by localized states.[4–7] A phenomenological model is presented which attempts to reconcile the steady-state ac photoconductivity results with those of time-of-flight measurements.

II. EXPERIMENTAL TECHNIQUES

The conductance and capacitance of thin films or crystal-platelet samples were measured, using either a 1615A General Radio capacitance bridge or a lock-in amplifier with a current-sensitive operational preamp. Most of the measurements were made at room temperature in the 20–10^5-Hz frequency range. Selected measurements were carried out over the 87–373 °K temperature range, using a programmable environmental test chamber. The samples were mounted in light-tight holders for dark-conductivity measurements. Photogenerated ac conductivity was measured by illumination of the samples through shutters mounted on the holders. A 100-*W* quartz-iodine lamp was used with the appropriate narrow bandpass filters, to ensure that the samples were illuminated by monochromatic bulk-absorbed light. In the case of amorphous selenium, where this is not possible, strongly absorbed 4000-Å-wavelength light was used. Both dark and photo ac measurements were done under steady-state conditions.

The amorphous Se and As_2Se_3 samples were made by thin-film evaporation on gold-covered glass substrates. Evaporated semitransparent gold electrodes were used on top. These chalcogenide films were in the 10–50-μm-thickness range. The polymeric films of the organic charge-transfer complex poly-(*N*-vinylcarbazole) (PVK) 2, 4, 7-trinitro-9-fluorenone (TNF) were cast from solution on a gold-covered glass plate. The samples were heated at 80 °C overnight to drive off the solvents. Semitransparent gold electrodes were again evaporated on top.

Single-crystal platelets, 0.6–0.8 mm in thickness, of insulating CdS were obtained from the Monsanto Co. Semitransparent indium electrodes on the (0001) face were used in this case. Layer-type crystals of As_2S_3 for microwave measurements were obtained by cleaving orpiment mineral crystals with transparent tape. Gold-electroded $(10\bar{1}0)$-face trigonal selenium crystals had been grown from a thallium-doped melt by the Czochralski technique. Polycrystalline trigonal selenium films were prepared by direct (thermal) conversion of amorphous selenium. Measurements were always done in the small-signal condition, with the ac field kept at $\leq 10^3$ V/cm.

Microwave measurements in the 9-GHz (X) band were made using a four-crystal balanced bridge, the signal arm of which was terminated in a TE_{103} reflection cavity. The four-crystal balanced bridge is commonly used in complex-reflection-coefficient plotting. When the phase of the microwave power in the bridge bias arm is properly adjusted, one set of crystals develops a signal voltage proportional to the real part of the cavity-arm reflection coefficient, while the other set provides an exactly out-of-phase signal, that is, one proportional to the imaginary part of the complex reflection coefficient. In these measurements the signal voltage proportional to the imaginary part of the reflection coefficient was used to drive an automatic frequency-control circuit so that the signal-crystal voltage was always maintained exactly proportional to the square root of the power absorbed by the sample in the cavity. The sample was illuminated by chopped monochromatic light from a prism monochromator through slits in the center of the narrow wall of the cavity. The sample was located in the maximum rf E field that is in the cavity's median plane. The signal voltage, amplitude modulated at the chopper frequency, was detected using a lock-in amplifier and the resulting signal was displayed as a function of incident wavelength on an xy recorder. Samples for microwave measurements were unelectroded films on quartz substrates, crystal platelets, or powders suspended in reagent-grade mineral oil.

III. RESULTS

A. Dark ac conductivity

The dark ac conductivity data we reported earlier[8] on the wide-band-gap chalcogenide glasses Se, As_2Se_3, and As_2S_3, while typical of a significant class of insulating materials, do not represent the universal behavior of either amorphous materials or of highly insulating crystalline solids.

Se, As_2Se_3, and As_2S_3 exhibit an ac conductivity proportional to ω^s where $s \lesssim 1.0$ in the 10^2–10^7-Hz frequency range. Microwave measurements indicate that the ac conductivity of these glasses saturates in the GHz range at values less than 10^{-4} Ω^{-1} cm^{-1}.

Figure 1 illustrates that similar behavior of the dark ac conductivity is observed in the 1 : 1 molar polymeric organic charge-transfer complex, formed from the donor poly-(N-vinylcarbazole) (PVK), and the acceptor 2, 4, 7-trinitro-9-fluorenone (TNF).[9] At 100 Hz, σ_{dark} $(= 10^{-12}\ \Omega^{-1}\ cm^{-1})$ is about two orders of magnitude higher than the dc conductivity measured at fields less than 10^4 V/cm. This suggests that the convergence of $\sigma(\omega)$ with the dc dark conductivity occurs in the 1-Hz region and is consistent with the linear behavior of σ_{dark} (ω) observed down to 20 Hz.

The results of dark-ac-conductivity measurements for single-crystal thallium-doped trigonal selenium, along with single-crystal CdS are shown in Fig. 2. At 100 Hz, their ac conductivities are nominally 10^{-6}, 10^{-10} Ω^{-1} cm^{-1}, respectively. For trigonal selenium and CdS the ac dark conductivity varied less than 30% over the 10^2–10^5-Hz frequency range. Single-crystal As_2S_3 also exhibited the ω^s, $s \sim 1$, type frequency dependence.[10]

B. ac photoconductivity

Figure 3 shows the interplay of the photoinduced ac conductivity, and the dark ac conductivity for As_2Se_3 at audio frequencies. At the lowest experimental frequencies the ac photoconductivity is between one order and two orders of magnitude higher than the dark ac conductivity. The light-induced

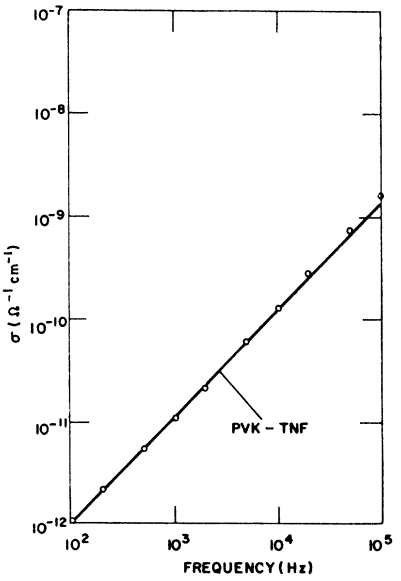

FIG. 1. Log-log plot of the dark ac conductivity $\sigma(\omega)$ of 1 : 1 PVK-TNF charge-transfer complex as a function of frequency.

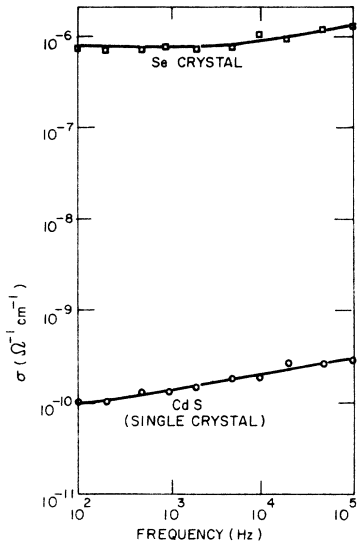

FIG. 2. Log-log plot of the dark ac conductivity $\sigma(\omega)$ of single-crystal CdS, and trigonal Se as a function of frequency.

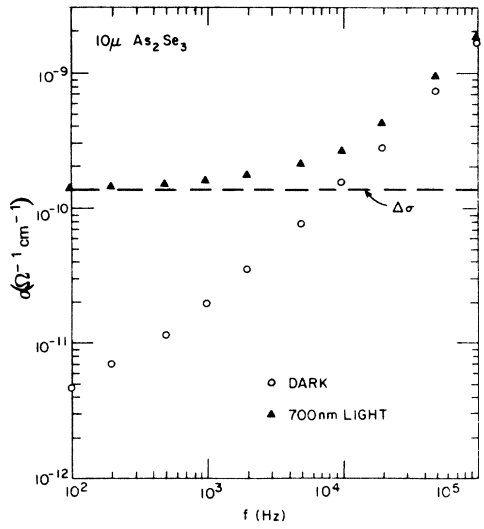

FIG. 3. Log-log plot of the dark ac conductivity and the ac photoconductivity of a-As_2Se_3 as a function of frequency. $\Delta\sigma = \sigma_{photo}(\omega) - \sigma_{dark}(\omega)$.

change in conductivity $\Delta\sigma = \sigma_{photo} - \sigma_{dark}$ is frequency independent and is plotted as a dashed line in the figure. As $\sigma_{dark}(\omega)$ increases with frequency, the quantity $\Delta\sigma/\sigma_{dark}$ becomes progressively smaller, that is, $\Delta\sigma$ is eventually lost in those noise components which are proportional to $\sigma_{dark}(\omega)$. The ac photoconductivity at low frequencies is nominally of the same order as the dc photoconductivity measured under the same irradiation conditions at low bias. Figure 4 illustrated that the same scheme is also already operative for the PVK: TNF complex at audio frequencies and mitigates against observation of high-frequency ac photoconductivity.

Similar results were obtained for the layer-crystal As_2S_3 and will be discussed in a forthcoming communication[10] on ac conductivity in molecular crystals. We wish to emphasize here only that single-crystal As_2S_3 does exhibit frequency-dependent dark ac conductivity and frequency-independent ac photoconductivity. Frequency-dependent ac conductivity is not restricted to amorphous solids or to single-crystal semiconductors measured at low temperature.

Figure 5 and the upper part of Fig. 6 illustrate the low-frequency behavior of crystalline CdS and trigonal selenium which do exhibit photomicrowave conductivity. In both cases σ_{photo} and σ_{dark} exhibit relatively mild frequency dependence; consequently $\Delta\sigma_{dark}$ is relatively constant and evidently remains so into the GHz frequency range.

The lower portion of Fig. 6 illustrates our results for amorphous selenium which represents a more complicated experimental situation because the ac photoconductivity was of necessity measured with strongly (surface) absorbed light.[11] In this case the sample sandwich was dielectrically inhomogeneous under illumination. The quantity $\Delta\sigma$ now has a restricted meaning in that light changes only the conductance of the sample, while σ_{photo} cannot be assigned to a bulk property. We nevertheless chose to present these data in much the same form, i.e., $\sigma_{photo} \equiv GL/A$, where G is the

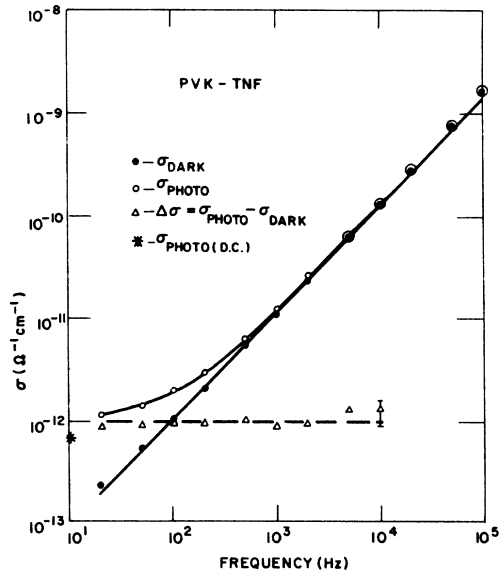

FIG. 4. Log-log plot of the dark ac conductivity and the ac photoconductivity of 1 : 1 PVK-TNF as a function of frequency.

conductance. The effect of space charge is, however, manifest in both the dispersive behavior of $\sigma_{photo}(\omega)$ at low frequencies and the corresponding reduction in its observed light intensity dependence in that frequency range.

Striking differences in the photomicrowave response of materials investigated in this study are entirely consistent with the behavior observed at much lower frequencies. Single-crystal insulating CdS exhibits strong photomicrowave conductivity. For the same nominal cavity filling factor and at the respective irradiation wavelengths for which As_2Se_3 and CdS exhibit comparable absorption coefficients, a photomicrowave signal is not observable in As_2S_3 even with 40-dB gain enhancement and long integrating time constants. Similarly, amorphous selenium and amorphous As_2Se_3 do not exhibit detectable photomicrowave response in our apparatus.[12,13] If, however, the amorphous selenium film is crystallized by heating to 140°C *in situ* using a variable temperature insert, photomicrowave signals become easily observable. These results stem from the fact that the ac dark conductivity and photoconductivity exhibit distinct frequency-dependent behavior.

IV. DISCUSSION

The dark ac conductivity of most of the insulators reported in Sec. III exhibit the ω^s behavior. It has been customary to explain this frequency dependence of $\sigma(\omega)$ in terms of a hopping-transport model. In particular it has been ascribed to phonon-assisted hopping between pairs of localized states.[1] While the simple "pair" model does indeed account for an ω^s dependence, the uniqueness of the model in explaining these results remains questionable. Both physically and mathematically, the hopping between pairs of sites is indistinguishable from a distribution of dipoles described by a Debye relaxation model. The general phenomenon of hopping transport *is distinct* in that it includes the possibility of both multisite hopping and finite dc current flow. Incorporation of these features gives rise to a different frequency dependence from that predicted by the pair model, when a sufficiently wide frequency range is considered. In addition, a fuller description of hopping can account more realistically for the temperature dependence of $\sigma(\omega)$. Thus to substantiate hopping as the dominant transport mechanism in these insulators it is important to understand the complete frequency and temperature dependence of $\sigma(\omega)$ in terms of a more general theory of ac hopping transport.[2] In particular, it is essential to be able to describe the T and ω dependence of the transition region where ω^s behavior changes to the dc limit behavior as well as the high-frequency region where $\mathrm{Re}\sigma(\omega)$ saturates. More complete measurements in these regions are being carried out and this comparison will be pursued in another study. It will suffice for this paper to consider hopping among localized states as being the main contribution to the dark ac conductivity.

In this context, the central issue, now, is to understand the ubiquitous flat frequency response of

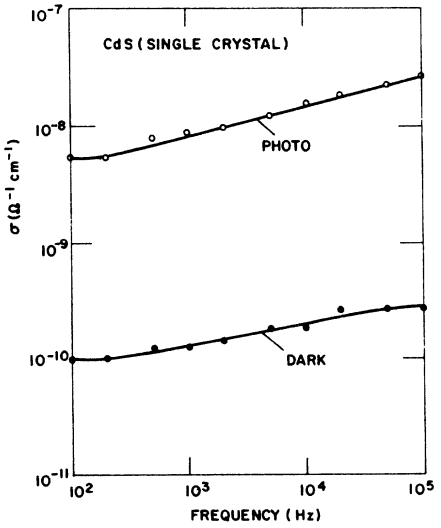

FIG. 5. Log-log plot of the dark ac conductivity and the ac photoconductivity of single-crystal CdS as a function of frequency.

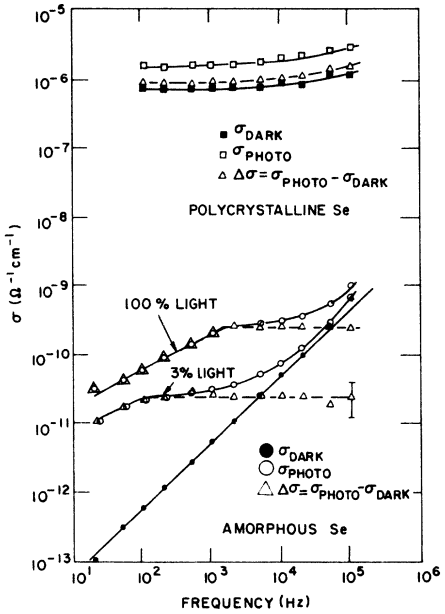

FIG. 6. Log-log plot of the dark ac conductivity and the ac photoconductance $G(\omega) \equiv \sigma_{photo}(\omega)\, A/L$ (see text) at two light levels of a-Se. The same plot for single-crystal trigonal Se.

the ac photoconductivity. This "understanding" must also dovetail with the results of transient, drift-mobility measurements made on these insulators.[14] In other words, any model involving various transport mechanisms and a density of states, for the ac measurements (with and without light), must be compatible with the transport picture obtained with the time-of-flight technique.

More specifically in PVK,[4] PVK-TNF,[5] and As_2Se_3,[7] the "anomalous" aspects of the dispersion in the transient photoconductivity can be naturally explained by assuming a stochastic or hopping motion of the charge carriers during their passage across the sample.[6] Steady-state ac photoconductivity in these materials, however, shows that $\mathrm{Re}\sigma(\omega)$ is independent of frequency until the dark conductivity dominates the power absorption with increasing ω.

We propose a simple model that reconciles these various transport features. We presume that the dark ac current is due to hopping among localized states, while in the presence of light the carriers are excited to some "extended" states,[15] which will be described in more detail below.

A. Steady-state photoconductivity

No discussion of electrical measurements in insulating materials can be separated from a detailed consideration of contact effects.[16] In the following we shall first describe steady-state photoconductivity in the absence of specific contact limitations. We then proceed to consider the dynamic effect of a blocking contact perturbation.

1. Neutral (Ohmic) contacts

Neutral contacts, by definition, simply replenish any carrier exciting the sample and moving into the external circuit. Therefore the contacts do not perturb bulk relations. In the steady-state condition the solution of the bulk kinetic equations for the carrier density is

$$\Delta n = g\tau_n \ , \tag{1}$$

where g is the generation rate and τ_n is the (microscopic) recombination lifetime. The expression in (1) is valid in the presence of an arbitrary number of trapping levels provided all recombination proceeds from the band state.[17] For the insulators under consideration one can assume $\Delta n \gg n_0$, the thermal equilibrium concentration (i.e., $\Delta n \simeq n$). The ac conductivity associated with this steady-state concentration in the extended states is

$$\sigma(\omega) = \sigma_0/(1 - i\omega\tau_M) \ , \tag{2}$$

where

$$\sigma_0 = eg\tau_n\mu_0 \ ; \tag{3}$$

τ_M is the momentum relaxation time related to the microscopic mobility μ_0 ($\mu_0 = e\tau_M/m_e$ for $\mu_0 \simeq 10$ $\mathrm{cm^2/V\,sec}$, $\tau_M \simeq 10^{-14}$ sec). We are assuming a unipolar conductivity (i.e., $\tau_p \ll \tau_n$, where τ_p is the recombination lifetime of the other sign carrier). For the entire frequency range used in the present investigation,

$$\omega\tau_M \ll 1 \ , \quad \sigma(\omega) \approx \sigma_0 \ . \tag{4}$$

2. Blocking contacts

Blocking contacts mean that the carrier is not replenished, although in most cases it can exit the sample. Thus we shall determine how the steady-state Δn in Eq. (1) can be perturbed if the contacts block carrier injection into the sample, but allow carriers to leave. First, we rewrite the photcurrent density corresponding to the σ_0 in (3) in terms of the transit time as

$$i_p = egL(\tau_n/t_\tau) \ , \tag{5}$$

where $t_\tau = L/\mu_0 E$ is the microscopic transit time and L is the interelectrode spacing.

The ratio τ_n/t_τ is usually taken to be the photoconductivity gain factor,[18] which can never be larger than unity for blocking contacts. One immediate question, therefore, is whether the expression for i_p in Eq. (5) is valid for the case of blocking contacts when $\tau_n > t_\tau$. The answer is no. This is determined simply by equating the rate of generation of carriers g to the *dominant* rate of loss (which, of course, establishes the steady-state condition). While excited the carriers travel a distance $\mu_0\tau_n E$, equal to the sum of the incremental distances traversed between trapping events. For $\tau_n > t_\tau$ this distance is greater than L, which means the carriers exit the sample before they are recombined, independent of any trapping. [It should be recalled that τ_n (in the steady state) is the *total* time a carrier spends in the "free" state, i.e., the total time as an excited carrier less any time spent in traps.[17]] Thus, the dominant rate of carrier loss, in this case, is the rate the carriers leave the sample, $\Delta n/t_\tau$. The steady-state carrier density is now given by

$$\Delta n = gt_\tau \ , \tag{6}$$

which results in the photocurrent

$$i_p = e\Delta nL/t_\tau = egL \ . \tag{7}$$

If, however, $\tau_n \ll t_\tau$, the carriers only manage to transverse a small fraction of L before recombination. The bulk loss mechanism is again the dominant one. Hence for the two limits (blocking contacts)

$$\begin{aligned} i_p &= egL\tau_n/t_\tau \quad \tau_n \ll t_\tau \ , \\ &= egL \qquad\ \ \tau_n > t_\tau \ . \end{aligned} \tag{8}$$

We shall refer to egL as i_e the emission-limited

TABLE I. ac steady-state photoconductivity ($\omega\tau_M \ll 1$).

Photocurrent i_p	Nature of contact	Relation of transit time and recombination time	Frequency
$egL\tau_n/t_\tau$	neutral	$\tau_n > t_\tau$ $\tau_n < t_\tau$	$\omega t_\tau >, < 1$
$egL\tau_n/t_\tau$	blocking	$\tau_n < t_\tau$	$\omega t_\tau >, < 1$
egL		$\tau_n > t_\tau$	$\omega t_\tau < 1$
$egL\tau_n/t_\tau$			$\omega t_\tau > 1$

current and note it is independent of all bulk transport parameters. Thus, strictly speaking, one can only discuss a σ_0 for blocking contacts when $\tau_n \ll t_\tau$. The preceding results are summarized in Table I.

3. *ac effects with blocking contacts*

In discussing steady-state photoconductivity with blocking contacts (as defined above), one determines that the transit time is a crucial variable. In relating the above analysis to the ac case one needs to consider the meaning of t_τ for an ac field. For an ac field with a rms amplitude of E_0, a t_τ can be established when

$$\omega < \pi \mu_0 E_0 / L \ , \tag{9}$$

i.e., when the half-period of the signal is greater than transit time appropriate to E_0. If $\omega t_\tau \gg 1$ then a typical carrier oscillates back and forth (with an out-of-phase factor determined by τ_M) and does not encounter the sample boundaries. In Fig. 7 we show schematically the frequency response of the photocurrent i_p for a case with $\tau_n > t_\tau$, blocking contacts and $\omega\tau_M \ll 1$. The ac effects on i_p are included in the summary in Table I.

B. Comparison of steady-state $\sigma(\omega)$ and transient $I(t)$ measurements

We propose that the frequency-independent part of the ac photoconductivity is due to σ_0 or i_e and that with increasing frequency the power dissipation is eventually dominated by the *independent* mechanism (hopping) of the dark conductivity.

If the dark conductivity is due to carriers in trap states, it can also be enhanced in the light. In fact, the ratio of free to trapped charge in the light should be approximately equal to the ratio in the dark. An examination of Fig. 3 indicates that the change in the free-carrier contribution due to the light is about a factor of 40. Experiments performed in the 100–373 °K temperature range show that the slight flattening in the dark ac conductivity at room temperature and 10^2 Hz represents the onset of a frequency-independent $\sigma_{dark}(\omega) \sim 2.5 \times 10^{-12}$ Ω^{-1} cm^{-1} for $\omega \lesssim 10$ Hz. One also observes the $\sigma_{photo}(\omega) \approx \sigma_{dark}(\omega)$ at $\omega \simeq 10^5$ Hz. If the carriers in the traps increased in the same ratio as the free

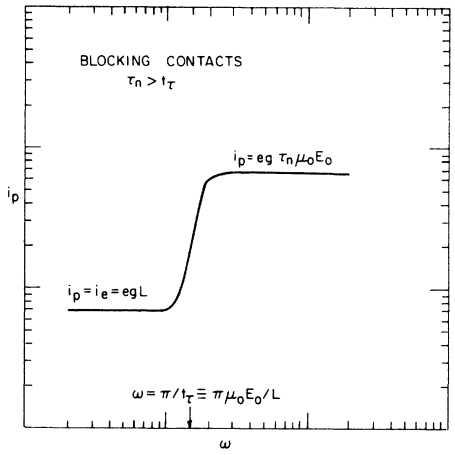

FIG. 7. Schematic log-log plot of the photocurrent of an insulator with blocking contacts and a recombination lifetime τ_n greater than the effective transit time $t_\tau = L/\mu_0 E_0$, as a function of frequency $2\pi\omega$.

carriers one should have $\sigma_{photo}(\omega) \approx (40)\sigma_{dark}(\omega)$ at the higher frequencies! The fact that this is not the case can be interpreted as increased evidence for $\sigma_{dark}(\omega)$ due to carriers hopping at the Fermi level (as suggested to us by E. A. Davis). That is, the number of carriers in the traps have changed but not the effective number at the Fermi level. Another possibility is that the carriers dominating $\sigma_{dark}(\omega)$ are in states corresponding to the recombination levels in the light. Although the number of carriers in trapping states can change, the steady-state population of the recombination centers is not expected to be modified.

Returning to a more immediate question we ask: If carriers promoted by light into extended states dominate the ac photocurrent, why do they not also (universally) dominate the transport of charge across the sample in a transient experiment? In the latter experiment a short pulse of strongly absorbed light "injects" one sign of carriers into the bulk (the sign depending on the applied field polarity). The measured current $I(t)$ monitors the drift of the carriers, and $I(t) \to 0$ as the carriers exit the sample or get captured into deep traps. The carriers in the deep traps can reappear as a contribution to $I(t)$ on a longer time scale. If carriers are promoted into the extended states but have a deep-trapping lifetime τ_D, much shorter than the transit time t_τ, then these carriers can be considered as highly range limited in regard to the transient measurement and do not contribute to $I(t)$ (except for a large spike at $t < \tau_D$). By definition, deep traps have a release time $\tau_R \gg t_\tau$ and τ_D need not coincide with τ_n the recombination lifetime. Thus in a steady-state ac (or dc) measurement a Δn can be

maintained in the extended states and dominate the power loss, while in a transient case the τ_D can be much shorter than the transit time (which can be established by carriers hopping in localized levels across the sample). In As_2Se_3 and PVF-TNF there is a convincing evidence that the $I(t)$ is indeed due to hopping.[4-7] To reiterate, *the transient measurement "selects" those carriers which individually transit the sample, while in the* ac *photoconductivity measurements described in this paper, the conductivity essentially monitors a steady-state population of carriers in the extended states (with short trapping lifetimes)*. With this framework now established, we shall examine each of the different materials below.

C. As_2Se_3

1. Bulk recombination

The conditions for the ac photoconductivity in As_2Se_3 shown in Fig. 3 correspond to weakly absorbed light $\alpha L \sim 1$, in a sandwich cell configuration with semitransparent gold contacts. For bulk-absorbed light

$$g = \eta \alpha I \ , \tag{10}$$

where η is the bulk quantum efficiency. The value of α at the peak of the band-pass filter (1.68 eV) is $\alpha \sim 10^3$ cm^{-1} and $I \sim 5\times10^{14}$ photons/cm^2 sec. It is deduced that gold contacts on As_2Se_3 are not neutral for applied fields $E > 3\times10^4$ V/cm because in this field range one can observe transient photoconductivity signals with strongly absorbed light.[19] It is not presently known whether gold contacts can be neutral for some lower field range such as the range $1-10^3$ V/cm used in the present measurements. Thus, there is some uncertainty about the nature of the contacts. In Table I we observe that for $\tau_n < t_\tau$ the relation (5) holds for i_p, both for neutral and blocking contacts. We shall *assume* (5) holds for As_2Se_3 and self-consistently deduce that $\tau_n < t_\tau$ and thereby justify our assumption. In contrast, if $\tau_n > t_\tau$ we would not know which expression for i_p in Table I is applicable unless we have more information about the behavior of the contacts.

The flat part of $\Delta\sigma$ in Fig. 3 has a value of 1.4×10^{-10} Ω^{-1} cm^{-1}. Using (10),

$$\Delta\sigma = 1.4\times10^{-10} = e\eta\alpha I \tau_n\mu_0 \ . \tag{11}$$

Thus

$$\eta\tau_n\mu_0 = 1.7\times10^{-9} \text{ cm}^2/\text{V} \ , \tag{12}$$

and for $\eta \simeq 0.08$ (which we discuss below),

$$\tau_n\mu_0 \simeq 10^{-8} \text{ cm}^2/\text{V} \tag{13}$$

for As_2Se_3. The relation $\tau_n < t_\tau$ can be rewritten

$$\tau_n\mu_0 E < L \ . \tag{14}$$

For $L = 10^{-3}$ cm and the value of $\tau_n\mu_0$ in Eq. (13) one observes that the inequality in Eq. (14) is true for $E \lesssim 10^5$ V/cm; a condition which is easily satisfied for the ac field range used in these measurements.

2. Quantum efficiency

The only source of quantum efficiency measurements available at present is transient $I(t)$ experiments.[20] Strongly absorbed light is used in these measurements and the number of carriers (holes) leaving the generation layer per photon can be determined. The total number of these carriers moving into the bulk or transport region can be effected by recombination in the generation layer. Thus we shall designate the composite quantum efficiency measured in a $I(t)$ experiment as a supply efficiency η_s, which need not coincide with the intrinsic η.

The supply efficiency η_s is observed to be field (E) and excitation wavelength (λ) dependent. For $\lambda \sim 500$ nm ($\alpha \sim 10^5$ cm^{-1}) the field dependence of $\eta_s(E)$ is linear below $E < 2\times10^4$ V/cm and above that field value $\eta_s \propto E^{1/2}$.

Preliminary measurements of dc bias field effects on the $\Delta\sigma$ in Fig. 3 show a saturation below $E \sim 5\times10^3$ V/cm and approximately $\Delta\sigma \propto E^{1/2}$ above this field. Until more detailed examination of dc bias effects on $\Delta\sigma$, as well as $\sigma_{\text{dark}}(\omega)$, which will be pursued in another study, has been completed, we assume the E dependence of $\Delta\sigma$ is due to η; i.e., $\Delta\sigma(E) \propto \eta(E)$. Now with this assumption it can be argued (as we do below) that η and η_s do coincide in the $E^{1/2}$ field-dependence region. The linear E dependence of $\eta_s(E)$, therefore, appears to be due to bulk recombination in the absorption layer.

We are now in a position to estimate η for the wavelength (700 nm) and field (6.25 V/cm) used in the measurement of the data in Fig. 3. The field 6.25 V/cm corresponds to the saturation region of $\Delta\sigma(E)$. For fields at $E \sim 10^5$ V/cm, $\Delta\sigma$ increases by a factor of 4. We have already stated that $\eta \simeq \eta_s$ in the high-field ($E \sim 10^5$ V/cm) or $E^{1/2}$ region. Transient measurements at 700 nm (with "thick" samples, $L \sim 60$ μm) indicate $\eta_s \simeq 0.3$ at $E = 1.5\times10^5$ V/cm. Therefore, since $\Delta\sigma(E) \propto \eta(E)$, the value of η in the saturation region is taken to be $(0.3)/4 \simeq 0.08$.

The value of $\tau_n\mu_0$ deduced from this analysis ($\tau_n\mu_0 \simeq 10^{-8}$ cm^2/V) supports a picture of bulk recombination effecting $\eta_s(E)$. Returning to the measurements of η_s at 500 nm, the field marking the transition from a linear to a square-root dependence of $\eta_s(E)$ is $E \sim 2\times10^4$ V/cm. At this field $\mu_0\tau_n E \simeq 10^{-4}$ cm, which is about a factor of 10 larger than the absorption depth ($\alpha^{-1} \sim 10^{-5}$ cm). Therefore, at fields below $E \sim 2\times10^4$ V/cm recombination effects should become increasingly important (i.e.,

$\mu_0\tau_n E \gtrsim \alpha^{-1}$) in η_s and it is reasonable to associate the linear E dependence with recombination in the absorption layer. At longer λ (corresponding to length α^{-1}) the linear part of η_s should cover a larger field range. There is preliminary evidence that this is indeed the case.[21]

A picture of η saturating at $E \lesssim 5\times10^3$ V/cm while the linear part of $\eta_s(E)$ includes recombination effects in the generation (absorption) layer[22] is numerically consistent with the value of $\tau_n\mu_0$ in (13) deduced self-consistently from $\Delta\sigma$. A summary of an over-all transport model of As_2Se_3 will be discussed in Sec. V.

D. PVK-TNF

In Fig. 4 the plot of the ac photoconductivity of the charge-transfer complex 1:1 molar PVK-TNF is remarkably similar to the results in As_2Se_3. One observes a merger of σ_{photo} with σ_{dark} for ($\omega/2\pi > 10^3$ Hz with a flat $\Delta\sigma$ corresponding to a value of 10^{-12} Ω^{-1} cm^{-1}, which is nearly equal to the dc photoconductivity (indicated by an asterisk in the figure). The idea of associating $\Delta\sigma$ with a steady-state number of carriers in extended states in the PVK-TNF may seem to need special explanation—especially because the (electron) transport is known to be a sensitive function of TNF concentration,[5,23] which indicates a hopping mechanism. However, the carriers in a steady-state photoconductivity measurement could be moving in an excited-state manifold of overlapping PVK-TNF complexes, with a very short range (*schubweg*). Another possibility, however, is that the photocurrent is i_e and therefore independent of the mobility. It should be recalled that, regardless of how the carrier moves, the i_e is established simply by virtue of the carrier living long enough to exit the sample and not be replenished by the contact. We therefore attempt the same analysis for PVK-TNF as we did for As_2Se_3 above. Equating $\Delta\sigma$ with $eg\tau_n\mu_0$ and inserting the values: $I \sim 10^{14}$ photons/cm^2 sec, $\alpha \sim 10^3$ cm^{-1} at $\lambda = 640$ nm, we obtain

$$6\times10^{-11}\ \text{cm}^2/\text{V} = \eta\mu_0\tau_n\ . \tag{15}$$

The value for η can be determined by a linear extrapolation of $\eta_s(E)$ measurements.[24,25] At the low-field end of the available data for the supply efficiency at $\lambda = 404.5$ nm, $\eta_s \simeq 3\times10^{-3}$ at $E \simeq 3\times10^4$ V/cm and further, $\eta_s(E)$, in this range, appears to have a linear field dependence. We choose as an upper limit $\eta \simeq 3\times10^{-4}$ at $E = 10^3$ V/cm, the amplitude of the ac field for the measurements in Fig. 4. Hence

$$\mu_0\tau_n \simeq 10^{-6}\ \text{cm}^2/\text{V}\ . \tag{16}$$

With this value $\mu_0\tau_n \simeq 10^{-3}$ cm $= L$ at $E = 10^3$ V/cm, thus we are dealing with a marginal case. At the highest experimental fields used the ac photocurrent most probably is i_e and the field dependence of the photocurrent would correspond to that of η. Also at these higher fields $\eta = \eta_s$. There is evidence that the I-V curve of PVK-TNF measured in a dc photoconductivity experiment at $E > 10^4$ V/cm indeed follows the field dependence of $\eta_s(E)$.[26]

E. Se

The ac photoconductivity measurements on amorphous Se shown in Fig. 6 are complicated by the fact that the sample is dielectrically inhomogeneous in the presence of light. There is a well-known energy gap between the onset of light absorption and significant photoconduction in Se.[11] Hence, with the sandwich cell geometry of the present measurements, strongly absorbed $\lambda = 400$-nm light ($\alpha \simeq 10^5$ cm^{-1}) was used. The steady-state condition therefore corresponds to a spatially inhomogeneous distribution of photoexcited carriers. The steady-state current in the bulk of the sample is clearly i_e, the emission limited current, with the absorption (or generation) layer as the source of supply. In this case the quantum efficiency η is undoubtedly the supply efficiency η_s. The conductivity σ_{photo} in Fig. 6 is, strictly speaking, (L/A) times (the photoconductance G). For such a layered dielectric one can observe frequency dispersion in G and indeed we attribute the low ω falloff in G_{photo} to a space-charge dispersion. The space-charge effect is consistent with the intensity dependence of this portion of G observed in the figure. With lower light levels (3%), corresponding to smaller space charge the falloff moves to lower ω. The flat ΔG is associated with the emission-limited current $i_e = e\eta_s I$ for this strongly absorbed case

$$\sigma E = 2\times10^{-8}\ A/\text{cm}^2 = en_s I\ . \tag{17}$$

The field $E = 75$ V/cm and the value $\sigma = G(L/A)$ at the 100% light level is 3×10^{-10} Ω^{-1} cm^{-1}. Inserting $I = 10^{14}$ photons/cm^2 sec we obtain $\eta_s \simeq 2\times10^{-3}$. This value of η_s agrees quite well with the value obtained by extrapolating the 400-nm data on η_s, obtained from transient measurements,[27,28] to the lower-field value of 75 V/cm. Thus the flat ΔG in amorphous Se is completely consistent with an emission-limited current. This is quite satisfying because for Se we establish the existence of a light-induced contact region which acts as a current source for the bulk of the solid.

F. Crystalline solids

In the insulating crystalline solids CdS and trigonal Se (Fig. 2 and the upper part of Fig. 6), and in the data on As_2S_3[9,10] one notes that ω^s dependence of the dark ac conductivity is not universal among highly insulating solids. The ac photoconductivity in single-crystal As_2S_3 is also similar to that observed in the amorphous materials we have been

considering.[9,10] The main feature of the ac photoconductivity of CdS and trigonal Se in Figs. 5 and 6, respectively, is the constant $\Delta\sigma$, even up to the microwave range.[29] The frequency independence of $\Delta\sigma$ is more pronounced than the dark conductivity, which is mildly dispersive in both crystalline materials.

In the context of the main study, in this paper, on amorphous insulators, one can now see the importance of making ac measurements on single-crystal insulators. They not only exhibit similar frequency and temperature dependencies in the ac conductivity (both with and without light) but they can serve as more carefully controlled models of some of the general features of conductivity we have discussed above. For example, CdS with *known* blocking contacts can illustrate the ac behavior shown schematically in Fig. 7. In addition, further materials work on As_2S_3 in connection with $\sigma_{dark}(\omega)$ can give us clues in our continuing analysis of $\sigma_{dark}(\omega)$ in amorphous insulators; i.e., the correlation of the purity (trap concentration) of As_2S_3 with the frequency dependence of σ_{dark}.

V. SUMMARY

We have made observations of the ac conductivity, with and without light, in a broad class of photoconducting materials. By measuring $\sigma(\omega)$ we can distinguish competing dissipative mechanisms by their characteristic frequency dependences. While we have not analyzed the nature of the carriers and electronic states which contribute to the $\sigma_{dark}(\omega)$ in detail, we have shown that in the presence of light a different set of carriers and/or states can dominate the power dissipation in some (lower) frequency range. The interaction of a frequency-dependent dark conductivity with a frequency-independent $\Delta\sigma$ is responsible for our inability to measure microwave photoconductivity in amorphous chalcogenides. We attribute the source of frequency-independent photoconductivity ($\Delta\sigma$) to either the low-frequency limit of the conductivity due to excited carriers moving in extended states (σ_0) or to an emission-limited current (i_e) which is independent of the bulk mobility. We have discussed the fact that different types of transport measurements tend to "select" different competing processes. In a transient photoconductivity experiment one essentially monitors the carriers drifting completely across the interelectrode distance, while in a steady-state measurement one samples a steady-state population of carriers, although each carrier can have an extremely short *schubweg*. Thus in As_2Se_3 one sees the outline of the following transport picture, the $\Delta\sigma$ in a dc or ac steady-state photoconductivity measurement can be associated with $\sigma_0 = eg\tau_n\mu_0$. The value $\tau_\eta\mu_0 = 10^{-8}$ cm^2/V is consistent with the field dependence of $\eta_s(E)$ (cf. end of Sec. IV C 2). The recombination centers in the generation layer using strongly absorbed light could correspond to the hopping sites in the bulk in a drift experiment.

In Se one establishes, in essence, an emission-limited current in the bulk due to the light-generated "contact" region. The value of η_s deduced from $\Delta\sigma$ is completely consistent with the η_s determined by charge integration techniques. Thus the flat $\Delta\sigma$ (apart from space-charge dispersion) can be attributed to i_e.

In PVK-TNF there is now evidence, from both our ac measurement and dc measurements of one of us,[26] that the current versus field shows a transition from a bulk- to an emission-limited current.

The consistency of the above ac measurements with both dc and transient measurements demonstrates the powerful extension ac techniques can provide in the understanding of the electrical properties of insulating materials. The ac techniques can, in addition, capitalize on experimental advantages such as high signal-to-noise ratio at relatively low signal levels, the shorter relaxation times available with low bias levels, and the freedom from contact limitations at sufficiently high frequency.

ACKNOWLEDGMENTS

We wish to thank J. Mort for suggesting the possible role of emission-limited currents i_e, and D. Pai for an elucidating discussion of the relation of i_e, the recombination time and the transit time in steady-state photoconductivity. We also wish to thank F. Knier and K. Pietrowski for help in sample preparation. We appreciate a critical reading of our manuscript by G. Pfister and R. Enck. We would like to thank R. Zallen and D. Blossey for providing the As_2S_3 crystals used in the microwave measurements and P. Vernon for supplying the trigonal Se crystal.

[1] M. Pollak and T. H. Geballe, Phys. Rev. 122, 1742 (1961); M. Pollak, Phys. Rev. 133, A564 (1964); M. Pollak, Phys. Rev. 138, A1822 (1965).

[2] H. Scher and M. Lax, Phys. Rev. B 7, 4491 (1973); H. Scher and M. Lax, Phys. Rev. B 7, 4502 (1973).

[3] L. N. Ionov, I. A. Akimov, and A. N. Terenin, Dokl. Akad. Navk SSSR 169, 550 (1966) [Sov. Phys. Dokl. 11, 599 (1967)].

[4] J. Mort, Phys. Rev. B 5, 3329 (1972).

[5] W. D. Gill, J. Appl. Phys. 43, 5033 (1972).

[6] E. W. Montroll and H. Scher, J. Stat. Phys. 9, 101 (1973); H. Scher and E. W. Montroll (unpublished); H. Scher, *Fifth International Conference on Amorphous and Liquid Semiconductors*, Garmisch-Partenkirchen, Federal Republic of Germany, 1973 (Taylor and Francis, London, 1974).

[7]M. E. Scharfe, Bull. Am. Phys. Soc. 18, 454 (1973).
[8]A. I. Lakatos and M. Abkowitz, Phys. Rev. B 3, 1791 (1971).
[9]A. I. Lakatos, M. Abkowitz, and D. F. Blossey, Bull. Am. Phys. Soc. 18, 361 (1973).
[10]M. Abkowitz, D. F. Blossey, and A. I. Lakatos (unpublished).
[11]J. L. Hartke and P. J. Regensburger, Phys. Rev. 139, A970 (1965).
[12]J. L. Stone, C. R. Haden, and S. A. Collins, J. Non-Cryst. Solids 8-10, 614 (1972).
[13]G. D. Arndt, W. H. Hartwig, and J. L. Stone, J. Appl. Phys. 39, 2653 (1968); W. H. Hartwig and J. J. Hinds, J. Appl. Phys. 40, 2020 (1969).
[14]An excellent review article describing the time-of-flight technique is W. Spear, J. Non-Cryst. Solids 1, 197 (1969).
[15]In this paper we choose to emphasize the conventional notion of an extended state; i.e., band state, and our analysis will proceed on this basis. Another possibility for the frequency independent contribution to $\sigma_{photo}(\omega)$ is spatially unrestricted hopping motion[2]; e.g., among band tail states. If this motion is not the type of *localized* carrier hopping associated with the ω^s-type behavior, then our analysis, applied to this case, although more specialized, remains, in principle, unchanged. Details of the conditions necessary to have frequency-independent hopping (at a finite frequency) will be pursued in another study.
[16]H. Scher, D. Pai, and J. Mort, J. Appl. Phys. 44, 2908 (1973).
[17]S. M. Ryvkin, *Photoelectric Effects in Semiconductors* (Consultants Bureau, New York, 1964), Chap. 6.
[18]A. Rose, *Concepts in Photoconductivity and Allied Problems* (Interscience, New York, 1963).
[19]M. E. Scharfe, D. Pai, and R. C. Enck (private communication).
[20]M. E. Scharfe, Phys. Rev. B 2, 5025 (1970); D. M. Pai and M. E. Scharfe, J. Non-Cryst. Solids 8-10, 752 (1972).
[21]M. E. Scharfe (private communication).
[22]The argument that precludes bulk recombination in the absorption layer in *a-Se* is based on the fact that such recombination centers would act as traps in the transport region in a transient measurement. See J. Mort, *Electronic and Structural Properties of Amorphous Semiconductors*, edited by P. G. LeComber and J. Mort (Academic, London, 1973), Chap. 15; such an argument is inapplicable in As_2Se_3, as the electron range *is* small.
[23]J. Mort and R. Emerald (unpublished).
[24]R. M. Schaffert, IBM J. Res. Dev. 15, 75 (1971).
[25]P. J. Melz, J. Chem. Phys. 57, 1694 (1972).
[26]A. I. Lakatos (unpublished).
[27]M. Tabak and P. Warter, Phys. Rev. 173, 899 (1968).
[28]D. M. Pai and S. W. Ing, Jr., Phys. Rev. 173, 729 (1968).
[29]Photomicrowave measurements on CdS are reported by J. Dziesiaty, Phys. Status Solidi 6, 913 (1964).